

Comparing morphologies of drainage basins on Mars and Earth using integral-geometry and neural maps

T. F. Stepinski¹ and S. Coradetti²

Received 26 April 2004; revised 29 June 2004; accepted 2 July 2004; published 4 August 2004.

[1] We compare morphologies of drainage basins on Mars and Earth in order to confine the formation process of Martian valley networks. Basins on both planets are computationally extracted from digital topography. Integral-geometry methods are used to represent each basin by a circularity function that encapsulates its internal structure. The shape of such a function is an indicator of the style of fluvial erosion. We use the self-organizing map technique to construct a similarity graph for all basins. The graph reveals systematic differences between morphologies of basins on the two planets. This dichotomy indicates that terrestrial and Martian surfaces were eroded differently. We argue that morphologies of Martian basins are incompatible with runoff from sustained, homogeneous rainfall. Fluvial environments compatible with observed morphologies are discussed. We also construct a similarity graph based on the comparison of basins' hypsometric curves to demonstrate that hypsometry is incapable of discriminating between terrestrial and Martian basins. **INDEX TERMS:** 1824 Hydrology: Geomorphology (1625); 1886 Hydrology: Weathering (1625); 5415 Planetology: Solid Surface Planets: Erosion and weathering; 6225 Planetology: Solar System Objects: Mars. **Citation:** Stepinski, T. F., and S. Coradetti (2004), Comparing morphologies of drainage basins on Mars and Earth using integral-geometry and neural maps, *Geophys. Res. Lett.*, 31, L15604, doi:10.1029/2004GL020359.

1. Introduction

[2] The interest in valley networks (VNs), the common features on Mars reminiscent of terrestrial river systems, remains high because the process of their formation has not been positively identified despite extensive studies. An initial focus has been on studying the planar morphology of the VNs themselves. While the integrated dendritic form of the VNs suggests formation by runoff [Masursky, 1973; Milton, 1973], many of their other planar attributes are inconsistent with runoff, but instead suggest groundwater sapping as the dominant formation mechanism [Pieri, 1980]. The advent of topographic data from the Mars Orbiter Laser Altimeter (MOLA) made possible more quantitative examination of VNs [Williams and Phillips, 2001; Aharonson et al., 2002; Stepinski et al., 2002], and, for the first time, enabled studies of their associated drainage basins.

[3] Drainage basins can be computationally extracted from topography data regardless of historical presence or

absence of runoff (T. F. Stepinski and M. L. Collier, Extraction of Martian valley networks from digital topography, submitted to *Journal of Geophysical Research*, 2004, hereinafter referred to as Stepinski and Collier, submitted manuscript, 2004). The morphology of the basin reflects the large-scale geology of the site, as well as its total fluvial degradation. The pattern of basin's degradation, and possibly the mechanism of that degradation, may be assessed from its morphology providing that the effects of geological setting can be factored out.

[4] Luo [2002] proposed the hypsometric curve as a representation of drainage basin morphology capable of distinguishing between runoff and groundwater sapping. Using a criterion based on hypsometric attributes, he has classified 194 Martian basins into 105 sapping-like, 42 fluvial-like, and 47 undetermined. The spatial intermingling of different classes of basins suggested a confusing mix of fluvial and sapping processes on Mars. Further studies by Fortezzo and Grant [2004] suggested that the hypsometric curve is sensitive to initial geological setting and thus a poor indicator of the style of erosion.

[5] In this paper we present the results of systematic comparison between morphologies of Martian and terrestrial drainage basins. This comparison was prompted by an observation that, at least in some cases, the relationship between the basin's morphology and its drainage network is strikingly different on the two planets. Figure 1 illustrates this difference. Panel A shows a drainage network drawn on the top of a topography for a drainage basin in Warrego Valles region on Mars. Panel B shows the same for the Green River drainage basin in Utah. Whereas in the Green River basin the drainage network conforms to the topography, in Warrego Valles the network appears to be disconnected from basin's topography. To investigate whether such disparity is typical we have undertaken a systematic comparison of Martian and terrestrial drainage basins. We employ two innovations to facilitate this comparison. First, we use the methods of integral-geometry to define a circularity function, a representation of basin morphology that is a better discriminant of the style of erosion than the hypsometric curve. Second, we use the self-organizing map, a neural net technique well-suited for a comprehensive comparison of different basins.

2. Methods

[6] We have used digital elevation data from the MOLA Mission Experiment Gridded Data Record (MEGD) [Smith et al., 2003] to construct digital elevation models (DEMs) of 26 Noachian sites featuring prominent valley networks. Martian DEMs have the resolution of 1/128 degree in both latitude and longitude. This corresponds to ~500 meters at the equator. Shuttle Radar Topography Mission (SRTM)

¹Lunar and Planetary Institute, Houston, Texas, USA.

²Department of Earth, Atmospheric and Planetary Science, Massachusetts Institute of Technology, Cambridge, Massachusetts, USA.

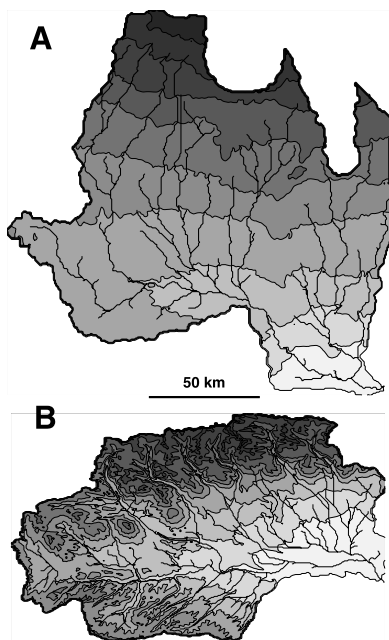


Figure 1. Same scale topographic maps of drainage basins in Warrego Valles, Mars (A) and Green River, Utah (B). Darker shades indicate higher elevations. Black lines represent drainage networks.

data with 90-meter resolution was used to construct DEMs of 27 sites in the United States and the South America featuring a variety of drainage systems. Subsequently, terrestrial DEMs were degraded to the 450-meter resolution for compatibility with Martian DEMs. A majority of terrestrial drainages are eroded by runoff. However, three of the selected terrestrial sites are located within the Atacama Desert of northern Chile, one of the driest places on Earth with the precipitation rate of $\sim 1\text{--}10$ cm/yr. These sites contain deeply incised, wide valley drainages (quebradas) that have been recently identified by *Hoke et al.* [2004] as groundwater sapping networks.

[7] Drainage basins on Earth and Mars are computationally extracted from DEMs using an algorithm developed for studies of terrestrial basins [Tarboton *et al.*, 1989]. Large, “contaminant” craters are removed from the basins using procedure described by Stepinski and Collier (submitted manuscript, 2004). Extracted Martian basins are labeled 1 to 26, and terrestrial basins are labeled 27 to 53 for use in Figures 3 and 4. Most of the basins on both planets have areas of the order of 10^4 km².

[8] We use the methods of integral-geometry morphological image analysis (IGMIA) to encapsulate a morphology of a drainage basin in a simple, yet informative and quantitative form. IGMIA [Michielsen and De Raedt, 2001] employs image functionals to assign numbers to the shape and connectivity of binary patterns. This method succinctly describes complex patterns and facilitates quantitative comparison between them. We “slice” the basin with a large number of horizontal planes located at progressively higher normalized elevations $0 \leq z \leq 1$. A given plane bisects basin’s pixels into those above and below the plane. A planar projection of all below-the-plane pixels forms a 2D pattern $\Omega(z)$. For this pattern we calculate two image functionals, its

area, $S[\Omega(z)]$, and its perimeter, $U[\Omega(z)]$. Aggregating values of these functionals from all different bisecting planes we construct the functions $S(z)$ and $U(z)$ that provide a quantitative characterization of a basin. Note that $S(z)$ is an inverse of the hypsometric curve.

[9] We have found that a function $\alpha(z) = 4\pi S(z)/U^2(z)$, which we call a circularity function, is a particularly useful descriptor of basin’s morphology. The circularity function reflects the change in the shape of the basin segment located below a given elevation as the elevation changes from its minimum (at the outlet) to its maximum (at the summit). The values of α range from 0 (extreme elongation) to 1 (circular shape). The value $\alpha(z = 1)$ is equal to the basin circularity. Whereas $S(z)$ measure the changes of basin’s area with the elevation, $\alpha(z)$ gauges the changes in basin’s shape with the elevation. These two integral-geometry measures are sensitive to different aspects of basin morphology. The new circularity function proved to be more suitable for distinguishing between different styles of erosion.

[10] To facilitate comparison between different basins, as represented by their circularity functions, we used the self-organizing map (SOM) technique [Kohonen, 1995]. The SOM is a computer-based neural network technique that groups similar, high dimensional input vector data into nearby points on a 2D map. Thus, SOM serves as a similarity graph for high dimensional data. The function $\alpha(z)$ is represented by an N-dimensional vector $[\alpha(z_1), \dots, \alpha(z_i), \dots, \alpha(z_N)]$, where $z_i = (i - 1)/(N - 1)$ is the set of equispaced elevation values. The SOM consists of a 2D regular grid of nodes (in our calculations we used 400 nodes arranged in a square grid) that, through a training procedure, evolves into a similarity map where similar α -vectors (representing basins) are associated with neighboring nodes.

3. Results

[11] Circularity functions have been calculated for all 53 basins. Figure 2 shows circularity functions for basins depicted in Figure 1. The shape of the circularity function for the Green River basin captures, in an abbreviated but clear fashion, the morphology of a landscape subjected to a sustained runoff. The interplay between production and transport of sediments results in a basin’s morphology that is characterized by elongation of the lower parts of the basin along the major streams. This brings about the conformance of drainage network and topography seen on the panel B of Figure 1. In terms of the integral-geometry, the low-laying segments of the basin have lower circularity than the entire

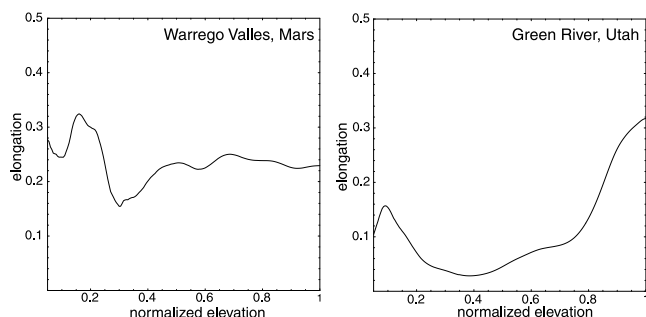


Figure 2. Circularity functions for Warrego Valles basin on Mars (left) and the Green River basin in Utah (right).

basin, resulting in the low values of $\alpha(z)$ for small relative elevations and increasing values of $\alpha(z)$ as $z \rightarrow 1$. The circularity functions for all 27 terrestrial basins have this characteristic shape, although they differ in details. For example, $\alpha(z)$ for the Green River basin indicates that this basin broadens at its lowest parts. This is attributed to an inclusion of a floodplain in the basin. Terrestrial basins have a wide range of overall shapes, but a narrow range of functional forms of $\alpha(z)$.

[12] The circularity function for the Warrego Valles basin does not display any systematic behavior, and, despite some localized fluctuations, stays approximately constant for the entire range of z . Thus, $\alpha(z)$ reflects well the featureless topography seen on the panel A of Figure 1. The morphology of this basin is fundamentally different from morphologies of terrestrial basins, and the shape of its circularity function bears no resemblance to the characteristic shape of terrestrial circularity functions. The forms of the circularity functions for the 26 Martian basins vary, but none shows terrestrial characteristics.

[13] Normalizing a circularity function using the whole basin circularity, $\alpha_n(z) = \alpha(z)/\alpha(1)$, disengages the internal basin morphology from the external basin shape. Two basins, possibly of different overall shapes, have similar α_n s if the relative changes of their shapes with elevations are similar. The overall shape of a basin reflects externally imposed geological setting. The normalization of α factors out this element allowing α_n to reflect erosional degradation.

[14] Figure 3 shows the α_n s similarity map constructed using the SOM algorithm. It serves as a proxy for basin morphologies similarity map, basins with similar morphologies are located close to each other on the map. Note that the SOM was trained using basins without indicating their planet of origin. After the map has been constructed we have marked the nodes associated with Martian basins as black circles and the nodes associated with terrestrial basins as white circles (white squares for the three basins located at the Atacama Desert). Addition of these labels to SOM's nodes reveals a clear dichotomy between Martian and terrestrial drainage basins. This dichotomy is further supported by the clustering of unlabeled nodes associated with the basins. Using Ward's hierarchical clustering method [Ward, 1963] we have found that these nodes can be best divided into just two clusters, one indicated on Figure 3 by the gray background and the other indicated by the white background. With few exceptions, the two clusters coincide with a division between Martian and terrestrial basins. Thus a natural binarity in the data corresponds to planet affiliation.

4. Discussion

[15] The similarity map (Figure 3) reveals a wide variety of basin morphologies on both Mars and Earth. This is indicated by a spread of both, terrestrial and Martian basins, over many different nodes in the SOM. In spite of this diversity, there is also a clear morphological distinction between the basins on the two planets. The terrestrial basins are located on the right side of the similarity map. The common factor of these basins, that transcends variations due to the local environment, is attributed to a characteristic imprint of runoff erosion on the landscape. Atypical terrestrial sites, such as the basins in the Atacama Desert, where

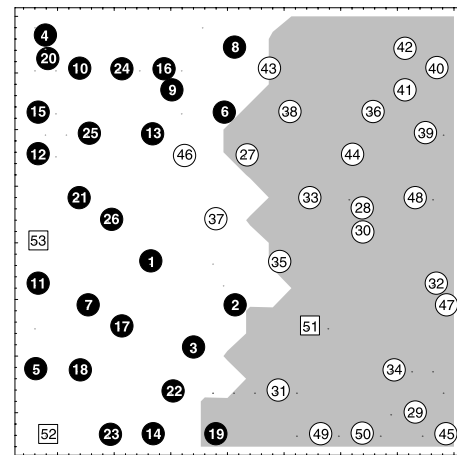


Figure 3. The SOM of Martian and terrestrial drainage basins based on normalized circularity functions. Martian basins are indicated by the black circles, terrestrial basins are indicated by the white circles (squares for the Atacama Desert basins). The two clusters derived by the Ward algorithm are shown as the white and gray backgrounds.

runoff is limited, defy this common pattern and are shifted to the left on the similarity map. The Martian basins are located on the left side of the similarity map. The common factor of these basins, that overcomes individual differences, appears to be a limited erosion of the basin outside the channels themselves.

[16] Does the dichotomy between basin morphologies on Mars and Earth preclude runoff as the dominant mechanism for erosion of Martian basins? Recently, *Irwin et al.* [2004] pointed out that runoff erosion on early Mars would be less efficient than on the Earth due to differences in a number of physical, climatic, and surficial properties between the two planets. They argued that, taking into account this inefficiency, properties of VNs, and, in particular, low values of drainage density on Mars, could be understood in term of runoff. A VN, the putative drainage network overlaying a basin, constitutes only a small part of the basin, where the presumed drain flow is concentrated. In the case of runoff, the remaining portion of the basin should also be eroded by a dispersed flow. Regardless of its efficiency, a sustained runoff would result in a characteristic basin's morphology that our method is capable of detecting. We don't find this "runoff signature" in any of the Martian basins that we have studied. Instead, Martian basins have their own characteristic imprint, qualitatively different from an imprint due to sustained runoff. Thus, we submit that the origin of VNs via the sustained, homogeneous precipitation is incompatible with our findings.

[17] Instead, our findings point to a fluvial environment characterized by heterogeneous and/or intermittent input of water into a basin. For example, the Atacama Desert basins, which are morphologically similar to Martian basins, are predominantly eroded by the water collected at an Altiplano located above the basins. Note that our results do not necessarily favor a groundwater sapping over the runoff as an erosion process. However, they favor a heterogeneous injection of water into the landscape. Groundwater sapping is one example of erosion that is compatible with a

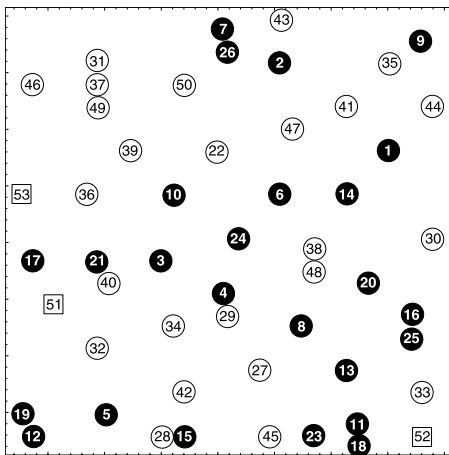


Figure 4. The SOM of Martian and terrestrial drainage basins based on hypsometric curves. See also legend for Figure 3.

heterogeneous injection of water into the landscape. Runoff from melting snowpacks provides another example of such environment. Carr and Head [2004] explored the possibility that valley networks formed as a result of melting snow that accumulated at low latitudes during sporadic periods of high obliquity. An example of an intermittent fluvial environment is transient warm and wet conditions initiated by large impacts [Colaprete et al., 2003]. Their computer simulations indicate that an impact of ~ 100 km object may produce rainfall accumulation of up to 400 cm scattered across the planet and lasting ~ 1 year. This mechanism would produce transient but approximately homogeneous precipitation on the length scale of the basins considered here. More work is needed to ascertain whether intermittency of precipitation alone is sufficient to account for an anomalous morphology of Martian basins.

[18] The concept of using the circularity function for characterization of drainage basins has application beyond the formation of Martian VNs. In the field of erosional topography the circularity function can be used for quantitative comparison between terrestrial basins in addition to existing methods such as the hypsometric analysis. Also, the idea of using the SOM for quantitative comparison of landforms transcends the specific application presented in this paper. In particular, the SOM can be used for comparison of basins on the basis of their hypsometric curves. Figure 4 shows the hypsometric curve similarity map constructed using the SOM algorithm. The functions $S(z)$, calculated for all 53 Martian and terrestrial basins are used to form the S -vectors that are fed to the SOM in a matter

fully analogous to the one described in section 3. Figure 4 clearly demonstrates lack of systematic differences between hypsometric curves for Martian and terrestrial basins supporting the findings of Fortezzo and Grant [2004].

[19] **Acknowledgments.** This research was conducted at the Lunar and Planetary Institute, which is operated by the USRA under contract CAN-NCC5-679 with NASA. This is LPI Contribution No. 1206.

References

- Aharonson, O., M. T. Zuber, D. H. Rothman et al. (2002), Drainage basins and channel incisions on Mars, *Proc. Natl. Acad. Sci. U. S. A.*, *99*, 1780–2783.
- Carr, M. C., and J. W. Head III (2004), Formation of Martian valley networks: Melting of low to mid-latitude snowpacks during periods of high obliquity?, *Lunar Planet. Sci.* [CD-ROM], XXXV, abstract 1183.
- Colaprete, A., R. M. Haberle, T. L. Segura et al. (2003), Post Impact Mars Climate Simulations using a GCM, *Int. Conf. Mars* [CD-ROM], VI, abstract 3281.
- Fortezzo, C., and J. A. Grant (2004), Hypsometric analyses of Martian basins: A comparison to terrestrial, lunar and Venusian hypsometry, *Lunar Planet. Sci.* [CD-ROM], XXXV, abstract 1647.
- Hoke, G. D., B. L. Isacks, T. E. Jordan, and J. S. Yu (2004), A groundwater-sapping origin of the giant quebradas of northern Chile, *Geology*, *32*(7), 605–608.
- Irwin, R. P., R. A. Craddock, and A. D. Howard (2004), Inefficient fluvial erosion and effective competing processes: Implication for Martian drainage density, *Lunar Planet. Sci.* [CD-ROM], XXXV, abstract 1991.
- Kohonen, T. (1995), *Self-Organizing Maps*, Springer-Verlag, New York.
- Luo, W. (2002), Hypsometric analysis of Margaritifer Sinus and origin of valley networks, *J. Geophys. Res.*, *107*(E10), 5071, doi:10.1029/2001JE001500.
- Masursky, H. (1973), An overview of geologic results from Mariner 9, *J. Geophys. Res.*, *78*, 4009–4030.
- Michielsen, K., and H. De Raedt (2001), Integral-geometry morphological image analysis, *Phys. Rep.*, *347*, 461.
- Milton, D. G. (1973), Water and processes of degradation in the Martian landscape, *J. Geophys. Res.*, *78*, 4037–4047.
- Pieri, D. C. (1980), Martian valleys: Morphology, distribution, age, and origin, *Science*, *210*, 895–897.
- Smith, D., G. Neumann, R. E. Arvidson et al. (2003), Mars Global Surveyor Laser Altimeter Mission Experiment Gridded Data Record, *NASA Planet. Data Syst. MGS-M-MOLA-5-MEGDR-L3-V1.0*, NASA, Washington, D. C.
- Stepinski, T. F., M. M. Marinova, P. J. McGovern, and S. M. Clifford (2002), Fractal analysis of drainage basins on Mars, *Geophys. Res. Lett.*, *29*(8), 1189, doi:10.1029/2002GL014666.
- Tarboton, D. G., R. L. Bras, and I. Rodriguez-Iturbe (1989), The analysis of river basins and channel networks using digital terrain data, *Tech. Rep. 326*, Ralf M. Parsons Lab. Mass. Inst. of Technol., Cambridge.
- Ward, J. (1963), Hierarchical grouping to optimize an objective function, *J. Am. Stat. Assoc.*, *37*, 236–244.
- Williams, R. M. E., and R. J. Phillips (2001), Morphometric measurements of Martian valley networks from Mars Orbiter Laser Altimeter (MOLA) data, *J. Geophys. Res.*, *106*, 23,737–23,752.

T. F. Stepinski, Lunar and Planetary Institute, 3600 Bay Area Boulevard, Houston, TX 77058, USA. (tom@lpi.usra.edu)

S. Coradetti, Department of Earth, Atmospheric and Planetary Science, Massachusetts Institute of Technology, 77 Massachusetts Avenue, Cambridge, MA 02139, USA. (scorad@mit.edu)